

## Dislocations in Submicron Grain Size and Nanocrystalline Copper

T. Ungár<sup>1</sup>, G. Tichy<sup>2</sup>, P. G. Sanders<sup>3</sup> and J. R. Weertman<sup>4</sup>

<sup>1</sup>Dept. of General Phys. and <sup>2</sup>Dept. of Solid State Phys.,

Eötvös University Budapest, H-1518, P.O.B. 32, Budapest, Hungary,

<sup>3</sup>Harvard University, 402 Gordon McKay, 9 Oxford St, Cambridge, MA, 02138 U.S.A.

<sup>4</sup>Dept. of Mater. Sci. and Eng., Northwestern University Evanston, IL, 60208 U.S.A.

### ABSTRACT

Using the dislocation model of strain anisotropy in X-ray diffraction peak profile analysis it is shown that in nanocrystalline copper produced by inert gas condensation dislocations are present, at least, down to average grain sizes of the order of 20 nm. Based on the analysis of the dislocation contrast factors it is suggested that with decreasing grain size the proportion of Lomer-Cottrell type dislocations increases.

### INTRODUCTION

The existence and type of dislocations in bulk nanocrystalline metals is still under debate [1-3]. High resolution electron microscopy indicates the presence of dislocations in the grain boundary regions, while the grain interior regions become clear of dislocations with decreasing grain size [4]. Using the method of X-ray diffraction peak profile analysis it was shown earlier that nanocrystalline copper produced by inert gas condensation does contain dislocations [5]. The previously used interpretation of X-ray data has been further developed and refined [6,7]. In the present work a series of copper specimens produced by inert gas condensation and deformed in some cases either by tension or compression will be analysed for the grain size, the grain size-distribution, the dislocation densities and the type of dislocations. Instead of the earlier suggested screw type it is found that as the grain size decreases the proportion of Lomer-Cottrell dislocations increases.

The evaluation of broadened X-ray diffraction peak profiles is based on the dislocation model of strain anisotropy [5]. This means that neither the FWHM (full width at half maximum) nor the integral breadth nor the Fourier coefficients of diffraction profiles are monotonous functions of the diffraction vector. A procedure has been developed to determine the crystallite size-distribution function and the dislocation structure in terms of the median and variance of a log-normal size-distribution and the density, the arrangement and the character (edge or screw type) of dislocations [6-8]. The FWHM, the integral breadths and the Fourier coefficients are analysed in terms of the *modified* Williamson-Hall and Warren-Averbach procedures.

### EVALUATION OF X-RAY DIFFRACTION EXPERIMENTS

The Fourier transform of diffraction peak profiles can be written in the form of the Warren-Averbach equation [9]:

$$\ln A(L) \cong \ln A_L^S - 2\pi^2 L^2 g^2 \langle \varepsilon_{g,L}^2 \rangle, \quad (1)$$

where  $A(L)$  are the absolute values of the Fourier coefficients of the physical profiles,  $A_L^S$  are the size Fourier coefficients,  $g$  is the absolute value of the diffraction vector and  $\langle \varepsilon_{g,L}^2 \rangle$  is the mean square strain in the  $g$  direction.  $L$  is the Fourier length,  $L=na_3$  [6], where  $a_3=\lambda/2(\sin\theta_2-\sin\theta_1)$ ,  $n$  are integers starting from zero,  $\lambda$  is the wavelength of X-rays and  $(\theta_2-\theta_1)$  is the angular range of the measured diffraction profile. In a dislocated crystal, for small  $L$  values,  $\langle \varepsilon_{g,L}^2 \rangle$  can be given as [10,11]:

$$\langle \varepsilon_{g,L}^2 \rangle \cong (\rho \bar{C} b^2 / 4\pi) \ln(R_e/L), \quad (2)$$

where  $\rho$ ,  $b$  and  $R_e$  are the density, the modulus of Burgers vector and the effective outer cut-off radius of dislocations, respectively. Peak broadening caused by dislocations depends on the relative orientations between the Burgers and line vectors of dislocations and the diffraction vector,  $\mathbf{b}$ ,  $\mathbf{l}$  and  $\mathbf{g}$ , respectively. This effect is taken into account by the dislocation contrast factors  $C$  [6,7,10-13]. In a texture free polycrystal or if the Burgers vector population on the different slip systems is random the  $C$  factors can be averaged over the permutations of the  $hkl$  indices [6]:

$$\bar{C} = \bar{C}_{h00} (1-qH^2), \quad (3)$$

where  $\bar{C}_{h00}$  are the average dislocation contrast factors for the  $h00$  reflections,  $H^2=(h^2k^2+h^2l^2+k^2l^2)/(h^2+k^2+l^2)^2$  and  $q$  is a parameters depending on the elastic constants of the crystal and on the edge or screw character of the dislocations [7].

$$\Delta K = 0.9/D + \alpha' (K\bar{C}^{1/2})^2 + O(K\bar{C}^{1/2})^4, \quad (4)$$

where  $K=2\sin(\theta)/\lambda$ ,  $\Delta K=2\cos(\theta)(\Delta\theta)/\lambda$ ,  $D$  is the apparent size parameter corresponding to the FWHM. It is obtained by extrapolation to  $K=0$  in the usual manner.  $O$  stands for higher order terms not interpreted here [14]. A similar equation can be given for the integral breadths and the corresponding apparent size parameter is denoted by  $d$  [8]. The *modified* Warren-Averbach equation is [5]:

$$\ln A(L) \cong \ln A^S(L) - \rho B L^2 \ln(R_e/L) (K^2 \bar{C}) + O(K^4 \bar{C}^2), \quad (5)$$

where  $B=\pi b^2/2$  and  $O$  stands for higher order terms, cf [14]. The size parameter corresponding to the Fourier coefficients, denoted by  $L_0$ , is obtained from the size Fourier coefficients  $A^S$  as described by Warren [9].  $d$  and  $L_0$  give the volume- and area-weighted mean column length, respectively [15,16]. A simple and pragmatic method has recently been developed to obtain the median and the variance,  $m$  and  $\sigma$ , of a log-normal size distribution of crystallites from the three apparent size parameters,  $D$ ,  $d$  and  $L_0$  [8]. For spherical crystallites with log-normal size distribution the area-, volume- and arithmetically-weighted mean crystallite sizes  $\langle x \rangle$  are [15]:  $\langle x \rangle_{\text{area}} = m \exp(2.5\sigma^2)$ ,  $\langle x \rangle_{\text{vol}} = m \exp(3.5\sigma^2)$  and  $\langle x \rangle_{\text{arithm}} = m \exp(0.5\sigma^2)$ , respectively.

## EXPERIMENTAL

Six different specimens are investigated: five specimens are bulk nanocrystalline copper prepared by inert gas condensation and hot compaction at Argonne National Laboratory [17]: O<sub>2</sub>, P<sub>2</sub> and N<sub>2</sub> in the as-prepared state and P<sub>2</sub> and N<sub>2</sub> after tensile and compression tests. The sixth specimen, denoted as V, has been prepared by equal channel angular compression (ECA) [18]. O<sub>2</sub> was measured twice: once after mechanical polishing and a second time after additional chemical etching. P<sub>2</sub> and N<sub>2</sub> were measured in the as-prepared state soon after synthesis and again after natural ageing at room temperature (RT) for about 9 months. P<sub>2</sub> and N<sub>2</sub> were measured also after tensile and compression tests, respectively. The mechanically tested P<sub>2</sub> and N<sub>2</sub> specimens were also measured in a second run after natural ageing RT. After ageing at RT, grain growth and/or recovery has been observed, especially in the undeformed P<sub>2</sub> and N<sub>2</sub> specimens. All different states of the specimens are listed in Table 1. The X-ray diffraction experiments were carried out by a special double crystal diffractometer with negligible instrumental peak broadening using a Nonius FR 591 Cu or Co rotating anode. More details are found in [9].

## RESULTS AND DISCUSSION

The FWHM of a bulk nanocrystalline (O<sub>2</sub>) and the ECA pressed (V) specimens (1a,b and 6 in Table 1.) are shown in the conventional Williamson-Hall plot [19] in Fig.1. The non-monotonous increase of the FWHM with  $K$  indicates strain anisotropy. The same data are shown in the *modified* Williamson-Hall plot according to eq. (4) in Fig. 2. The best fitting  $q$  values according to eq. (3) are indicated in the figure. In the case of the bulk nanocrystalline specimen (open circles and squares) stacking faults were also taken into account, as in [5]. The very different  $q$  values are in accordance with the very different strain anisotropy visualized qualitatively by the horizontal solid and slanted dashed lines in Fig. 1. passing through the FWHM of the 200, 220 and 222 reflections, respectively. From the three apparent size parameters,  $D$ ,  $d$  and  $L_0$ , obtained by using eqs. (4) and (5) for the FWHM, the integral breadths and the Fourier coefficients of profiles, the median and the variance,  $m$  and  $\sigma$ , of the log-normal crystallite size-distribution have been determined. The values of  $q$ ,  $\sigma$ ,  $m$  and  $\langle x \rangle_{\text{vol}}$  for the investigated specimens are given in Table 1. Typical errors of the data are indicated in a few cases. The  $m$  and  $\langle x \rangle_{\text{vol}}$  values show that RT exposure of some of the samples for a period of about 9 months led to increase in the mean grain size. The increase of the variance in the same cases indicate the widening of size distribution and a heterogeneous grain growth. TEM grain size measurements of the same specimens are in good correlation with the present results [20].

The  $q$  parameter [see eq. (3)] is plotted vs. the arithmetic average crystallite size  $\langle x \rangle_{\text{arithm}}$  in Fig. 3. The TEM grain size measurements of the same specimens [20] have shown that the X-ray and TEM results are in closer agreement for finer grain size. In the following the finer grain size region will be discussed therefore the term grain will be used instead of crystallite. In the figure it can be seen that as the grain size decreases the value of  $q$  increases. The line through the measured data is to guide the eye and the vertical line at 200 nm is a typical error bar. The values of  $q$  were calculated numerically as a function of the elastic anisotropy  $A_z = 2c_{44}/(c_{11} - c_{12})$ , where  $c_{ij}$  are the elastic constants of the crystal, for Burgers vectors:  $\mathbf{b} = a/2\langle 110 \rangle$ ,  $\mathbf{b} = a/2\langle 111 \rangle$  and  $\mathbf{b} = a/2\langle 100 \rangle$  in cubic crystals. For  $\mathbf{b} = a/2\langle 110 \rangle$  edge or screw dislocations, the  $q$  values are plotted vs.  $A_z$  in Fig. 4. In the case of edge dislocations they depend slightly on the ratio  $c_{12}/c_{44}$ .

For copper  $A_z=3.21$ . The vertical line in the figure shows that for dislocations with these Burgers vectors the  $q$  parameter values in copper vary between 1.68 and 2.37. For dislocations with Burgers vectors  $\mathbf{b}=a/2\langle 111 \rangle$  this range is between 1.60 and 2.68 [7].

Next the  $q$  values of  $\langle 100 \rangle$  type dipoles will be evaluated. The displacement field between the two dislocations of a dipole is homogeneous. For homogeneous strain  $q_{\text{hom}}$  is:

$$q_{\text{hom}} = 3 - [(\epsilon_{xx} + \epsilon_{yy} + \epsilon_{zz})^2 + 4(\epsilon_{xy}^2 + \epsilon_{yz}^2 + \epsilon_{zx}^2)] / (\epsilon_{xx}^2 + \epsilon_{yy}^2 + \epsilon_{zz}^2), \quad (6)$$

where  $\epsilon_{ij}$  is the strain tensor. Assuming that the dislocation lines are in the  $z$  direction in a cartesian coordinate system the strain tensors for the two possible dipole configurations perpendicular to each other are: (i)  $\epsilon_{xx} = -\epsilon_{yy} = (1+\nu)b/\delta$ ;  $\epsilon_{zz} = 0$  or (ii)  $\epsilon_{xx} = \nu b/\delta$ ;  $\epsilon_{yy} = -b/\delta$ ;  $\epsilon_{zz} = \nu b/\delta$ , where  $\nu$  is Poisson's ratio and  $\delta$  is the separation of the dipoles. Poisson's ratio for the  $\langle 100 \rangle$  direction in copper is:  $\nu = 0.42$  [21]. Using eq. (6) it can be shown that for the two dipole configurations: (i)  $q_{\text{hom}} = 3$  and (ii)  $q_{\text{hom}} = 2.981$ . In both cases, the  $q$  values for the  $\langle 100 \rangle$  type dipoles are practically 3.

On the basis of the above considerations the following mechanism is suggested for the increase of the  $q$  parameter with decreasing grain size. The  $\langle 100 \rangle$  type dipoles consist of Lomer-Cottrell sessile locks which are well known to be present in the dislocation structure in copper. As long as the average grain size is above a certain limit the overwhelming fraction of the dislocation density is of the usual dislocations with Burgers vectors  $\mathbf{b}=a/2\langle 110 \rangle$ . In this case the value of  $q$  is in the range corresponding to these dislocations, since the few Lomer-Cottrell locks do not contribute much to this average value. As, however, the grain size decreases, the  $\langle 110 \rangle$  type mobile dislocations move to the grain boundaries where they annihilate by the usual mechanisms. The sessile Lomer-Cottrell locks can more successfully survive this annihilation mechanism. As a result the fraction of the Lomer-Cottrell locks in the total dislocation density increases with decreasing grain size. The increase of the  $q$  value with decreasing grain size indicates the increase of the volume fraction of Lomer-Cottrell locks in the entire dislocation structure. The model still has to be verified by TEM investigations.

Table 1. The values of  $q$ ,  $\sigma$ ,  $m$  and  $\langle x \rangle_{\text{vol}}$  for the different specimens ( $\langle x \rangle_{\text{vol}}$  is the volume averaged particle size)

Specimen	$q$	$\sigma$	$m$ [nm]	$\langle x \rangle_{\text{vol}}$ [nm]
1a. O <sub>2</sub> , mechanical polish	2.69±0.1	0.7±0.02	6.6±0.2	29
1b. O <sub>2</sub> , +chemical etching	2.61	0.7	6.6	29
2a. P <sub>2</sub> , as-received	2.13	0.62	22	68
2b. P <sub>2</sub> , undeformed +9 m at RT	2.0	1.15	5.2±0.5	207
3a. N <sub>2</sub> , as-received	2.1	0.64	22	77
3b. N <sub>2</sub> , undeformed +9 m at RT	2.1	0.84	9.5±0.5	87
4a. P <sub>2</sub> , tensile deformed	2.47	0.58	17	45
4b. P <sub>2</sub> , tensile deformed +9 m at RT	2.34	0.73	9.8	49
5a. N <sub>2</sub> , compression deformed	2.3	0.69	13.5	59
5b. N <sub>2</sub> , compression deformed + 9 m at RT	1.9	0.79	13.5	87
6. V, deformed by ECA	1.96	1.06	11.8	307

## CONCLUSIONS

Based on X-ray diffraction peak profile analysis of nanocrystalline and submicron grain size copper specimens it is suggested that with decreasing grain size the surviving type of dislocations are most probably the  $\langle 100 \rangle$  type Lomer-Cottrell locks.

## ACKNOWLEDGEMENTS

Thanks are due to Mr G. Ribárik and Dr J. Gubicza for their kind assistance in evaluating the size distribution functions. T.U. is grateful to the Hungarian Scientific Research Fund, OTKA, Grant Nos. T031786, T029701 and AKP 98-25 2,2.

## REFERENCES

1. A. H. Chokshi, H. Gleiter and A. R. Rosen, *Scripta Metall.* **23**, 1679 (1989).
2. H. Van Swygenhofen and A. Caro, *Nanostr. Mater.* **9**, 669 (1997).
3. J. R. Weertman, D. Farkas, K. Hemker, H. Kung, M. Mayo, R. Mitra and H. Van Swygenhofen, *MRS Bull.* **24**, 44 (1999).
4. T. Braisaz, P. Ruterana, G. Nouet, Ph. Komninou, Th. Kehagias, Th. Karakostas, P. Pouloupoulos, M. Aggelakeris, N. Flevaris and A. Serra, *This Solid Films*, **319**, 140 (1998).
5. T. Ungár, S. Ott, P. G. Sanders, A. Borbély and J. R. Weertman, *Acta mater.* **46**, 3693 (1998).
6. T. Ungár and G. Tichy, *phys. stat. sol. (a)*, **147**, 425 (1999).
7. T. Ungár, I. Dragomir, Á. Révész and A. Borbély, *J. Appl. Cryst.* **32**, 992 (1999).
8. T. Ungár, J. Gubicza and G. Ribárik, *J. Appl. Cryst.* submitted for publication.
9. B. E. Warren, *Progr. Metal Phys.* **8**, 147 (1959).
10. M. A. Krivoglaz, in *Theory of X-ray and Thermal Neutron Scattering by Real Crystals*, Plenum Press, N. Y. 1969; and in *X-ray and Neutron Diffraction in Nonideal Crystals*, Springer-Verlag, Berlin Heidelberg New York, 1996.
11. M. Wilkens, *phys. stat. sol. (a)* **2**, 359 (1970).
12. M. Wilkens, *phys. stat. sol. (a)*, 1987, **104**, K1.
13. R. Kuzel Jr. and P. Klimanek, *J. Appl. Cryst.* 1989, **22**, 299.
14. I. Groma, *Phys. Rev. B*, **57**, 7535 (1998).
15. W. C. Hinds, *Aerosol Technology: Properties, Behavior and Measurement of Airborne Particles*, Wiley, New York. (1982).
16. J. I. Langford, D. Louer and P. Scardi, *J. Appl. Cryst.* **33**, 964 (2000).
17. P. G. Sanders, G. E. Fougere, L. J. Thompson, J. A. Eastman, and J. R. Weertman, *Nanostruct. Mater.*, **8**, 243 (1997).
18. R. Z. Valiev, E. V. Kozlov, Yu. F. Ivanov, J. Lian, A. A. Nazarov and B. Baudelet, *Acta metall. mater.* **42**, 2467 (1994).
19. G. K. Williamson and W. H. Hall, *Acta metall.* **1**, 22 (1953).
20. R. Mitra, T. Ungár, T. Morita, P. G. Sanders and J. R. Weertman, in *Advanced Materials for the 21st Century*, Eds. Y. W. Chung, D. C. Durand, P. K. Liaw, G. B. Olson, TMS, Warrendale, PA, 1999, p. 553.
21. R. F. S. Hearmon, in *Landolt-Börnstein*, **1**, pp. 1-39 (1966).

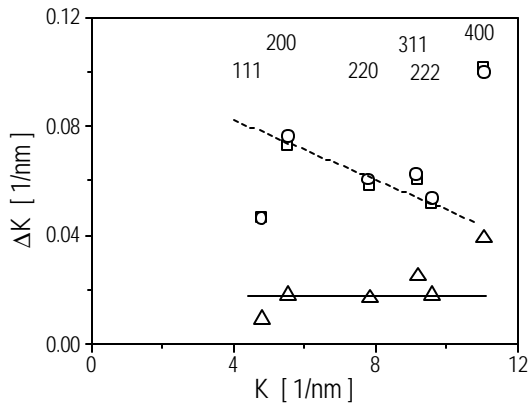


**Figure 1.** Conventional Williamson-Hall plot of the FWHM of a bulk nanocrystalline ( $O_2$ , open circles after polishing, open squares after additional chemical etching) and the ECA pressed (V, open triangles) specimens. The horizontal solid- and slanted dashed lines go through the FWHM of the 200, 220 and 222 reflections, respectively.

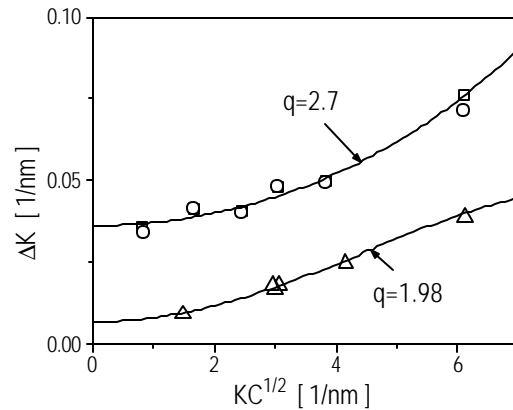


**Figure 2.** The same data as in Fig. 1, plotted in the modified Williamson-Hall plot. The best fitted  $q$  values in eq. (3) are indicated in the figure. The solid lines are the best fitted curves according to eq. (4).

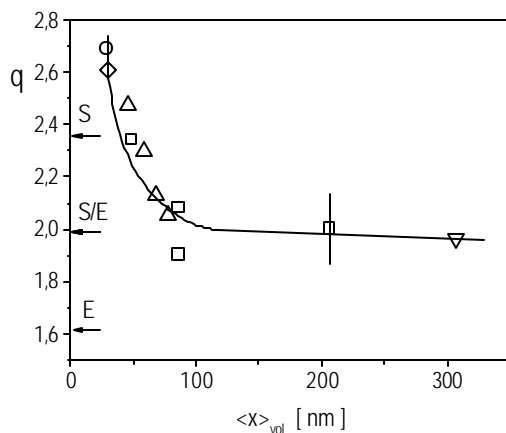


**Figure 3.** The experimentally determined  $q$  values vs. the volume averaged crystallite size. The symbols according to Table 1. are: open circle and diamond: 1a, 1b; open up-triangle: 2a, 3a, 4a, 5a; open square: 2b, 3b, 4b, 5b; open down-triangle: 6. S, S/E and E stand for screw, screw/edge and edge dislocations, respectively.

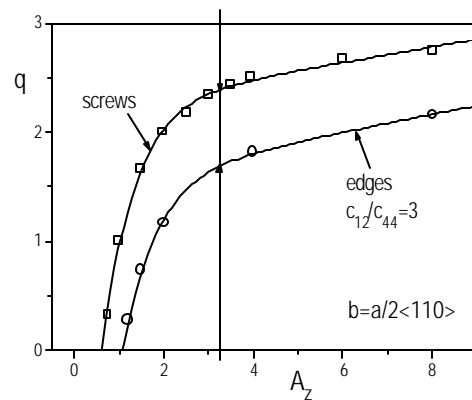


**Figure 4.** The variation of the  $q$  parameter [see eq. (3)] as a function of the elastic anisotropy (or the Zener constant)  $A_z$  in an fcc crystal for dislocations with  $\mathbf{b}=a/2\langle 110 \rangle$  Burgers vectors [7].